Journal of Photochemistry, 10 (1979) 205 - 213

TRIPLET STATE DEACTIVATION AND PHOTOCHEMISTRY OF AROMATIC THIOKETONES IN SOLUTION: XANTHIONE

U. BRUHLMANN and J. ROBERT HUBER
Fachbereich Chemie, Universität Konstanz, D-7750 Konstanz (F.R.G.)
(Received April 12, 1978; in revised form June 7, 1978)

Summary

The decay of triplet xanthione has been studied by means of the phosphorescence decay kinetics and the photodecomposition quantum yields ϕ_X measured in a variety of solvents at room temperature. Both the triplet decay and ϕ_X are strongly dependent not only on the solvent but also on the xanthione concentration. Based on these results a mechanism for the photochemical transformation of xanthione is proposed which features a primary photochemical step involving hydrogen abstraction from the solvent and the formation of a solvent-caged radical pair. Following these steps there is a competition between the recombination of the caged radicals and the reaction of the thioketyl radical with a xanthione ground state molecule. The reaction scheme is supported by quantitative calculation of the yields.

1. Introduction

Thiocarbonyl compounds are photochemically active not only in their lowest triplet state (T_1, $n\pi^*$) but, often, also in their second excited singlet state (S_2, $\pi\pi^*$). The major photochemical reactions which originate from these excited states are the photoreduction by hydrogen abstraction from appropriate solvents and cycloaddition. Both of these photoreactions of thiones are well documented and have been the subject of recent reviews [1, 2] and publications [3 - 6].

Xanthione, an aromatic thioketone, has proved to be particularly suitable for studying the photophysical properties of thiones [7, 8]. Recently, the triplet state and the intersystem crossing process of this molecule have been investigated by means of the optically detected magnetic resonance technique [9], and triplet lifetimes have been measured under a variety of conditions. It was shown that quenching of the triplet state by ground state xanthione molecules is diffusion controlled. This process, which is evidently physical in nature, probably involves triplet excimer formation [10].

Substantial information is now available about the xanthione triplet (T_1) state. The observation that T_1 is the only important photoactive state makes xanthione particularly suitable for a mechanistic study of the photochemical transformations of aromatic thioketones in solution.

The salient experimental findings about xanthione photochemistry are consistent with a primary photochemical step which involves hydrogen abstraction from the solvent and furnishes a solvent-caged radical pair. Following this step there is a competition between the recombination of the caged radicals and the reaction of the thioketyl radical with a xanthione ground state molecule which, after further reactions, ultimately yields stable photoproducts. This sequence of events is supported by computer simulation of the course of the reaction.

2. Experimental

Xanthione (X), which was synthesized by a published procedure [11], was repeatedly recrystallized from ethanol (m.p. 155 - 150 °C). 3-Methylpentane (3-MP, purum, Fluka AG) was purified by three cycles of frontal chromatography over Al_2O_3 (neutral, Merck AG) just prior to its use. Ethanol-d_1 (minimum degree of deuteration 99%, Merck AG), ethanol-d_6 (minimum degree of deuteration 99%, NMR spectroscopy grade, Merck AG) and all other solvents were used as received.

The quantum yield ϕ_X of xanthione photodecomposition was determined spectrophotometrically by use of a ferrioxalate actinometer [12]. The photolyses were performed with 1.5×10^{-4} M xanthione solutions, with excitation into the $S_2 \leftarrow S_0$ absorption band (ϵ(24 630 cm^{-1}) = 14 800 M^{-1} cm^{-1} in ethanol). For this purpose a 150 W high pressure xenon arc lamp (Osram) was employed in combination with a Spex Minimate monochromator. The band-pass of the excitation light was ± 50 Å, and intensities were about 10^{14} photons cm^{-2} s^{-1}. The irradiation time of the degassed or deoxygenated samples was limited so that no more than about 15% of the initial xanthione molecules underwent decomposition.

The phosphorescence decay times were measured with a nitrogen laser (Lambda Physik, Model 100A) excitation source. The lifetime analyses and the reaction simulations were performed with a PDP 11/40 minicomputer.

3. Results

The lifetime of the reactive triplet state of X at room temperature is concentration- and solvent-dependent. The triplet decay constants k_0 at infinite dilution were determined for a series of solvents by means of plots based on the Stern–Volmer relation:

$$k_m = k_0 + k_Q[X_0]$$

TABLE 1

Rate constants and photodecomposition quantum yields of xanthione at room temperature[a]

Solvent	$k_0 \times 10^{-5}$ [b] (s^{-1})	$k_Q \times 10^{-9}$ ($M^{-1}\ s^{-1}$)	ϕ_X [c]	τ (77 K) (μs)
MCH	2.0	8.7	0.014	40
Acetonitrile	3.6	13	$< 5 \times 10^{-4}$	
3-MP	3.7	17	0.005	40
Methanol	7.6	9.7	0.001	
Ethanol	11	6.2	0.15	41
i-PrOH	22	1.9	1.3	
Ethanol-d_1	8.2	6.0	0.14	46
Ethanol-d_6	8.3	5.9	0.009	55

[a] Estimated error: k_0, k_Q, $\tau \approx \pm 5\%$; $\phi_X \approx \pm 10\%$.
[b] Extrapolated to infinite dilution.
[c] Initial xanthione concentration, 1.5×10^{-4} M.

In this equation k_m is the measured triplet decay constant at finite concentration and k_Q the rate constant for physical quenching between xanthione T_1 and ground state molecules. As listed in Table 1, the k_0 values are significantly larger in alcoholic solvents than they are in aprotic solvents [7]; in the former they increase in the order methanol < ethanol < isopropyl alcohol. Moreover, in ethanol and isopropyl alcohol (i-PrOH) solutions the largest k_0 as well as ϕ_X values were measured.

The photodecomposition of X at room temperature is also strongly dependent on the xanthione concentration. Figures 1 and 2 show this dependence for ϕ_X in ethanol and in methylcyclohexane (MCH). In ethanol, ϕ_X increases steadily to a concentration of approximately 5×10^{-5} M, reaches a maximum at approximately 6×10^{-5} M and then decreases slowly as the concentration is further increased. The behaviour in MCH is similar.

The quantum yield was found to be independent of the incident light intensity between 10^{13} and 10^{15} photons $cm^{-2}\ s^{-1}$. In contrast to fluid solutions, no appreciable photodecomposition of X is observed in glassy ethanol (or in ether–isopentane–ethanol (EPA)) at 77 K or in a Plexiglass matrix at room temperature.

The deuterium effect for k_0 and ϕ_X was determined in ethanol-d_1 and ethanol-d_6 solutions. In both solvents the k_0 values are not significantly altered with respect to those in ethanol (Table 1). However, the decomposition quantum yield is dramatically reduced by a factor of about 16 in going from ethanol to ethanol-d_6. Between ethanol and ethanol-d_1, ϕ_X is unchanged within experimental error.

Mass spectrometric analysis of the photoproducts in degassed ethanol and 3-MP solutions reveals a strong peak at $m/e = 181$. For an ethanol-d_6 solution this peak is detected at $m/e = 182$. An additional peak at mass 166, which appears for photolyses performed in a cyclohexane solution, is attributed to the bicyclohexyl radical.

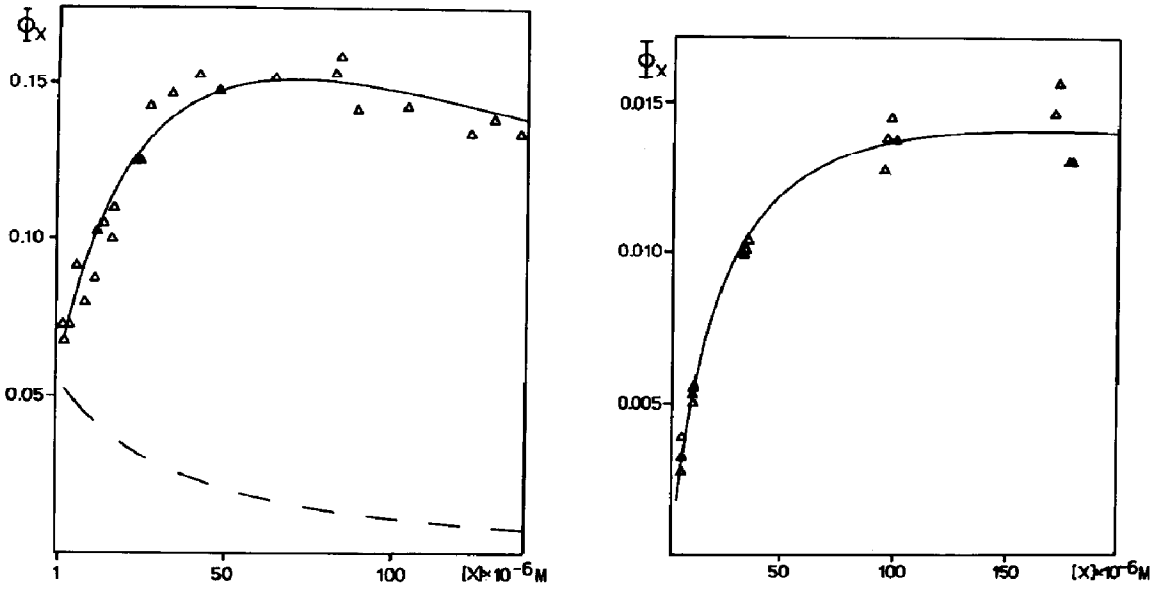

Fig. 1. Photodecomposition quantum yield of xanthione as a function of xanthione concentration in ethanol. The solid line represents the results of a computer simulation of eqn. (8) with the following rate constants: $k_H = 1.1 \times 10^4$ M^{-1} s^{-1}; $k_Q = 6.2 \times 10^9$ M^{-1} s^{-1}; $k_0 = 1.1 \times 10^6$ s^{-1}; $k_{R2} = 6.0 \times 10^9$ M^{-1} s^{-1}; $k_{R1} = 6.0 \times 10^3$ M^{-1} s^{-1}; $k_- = 1.7 \times 10^5$ s^{-1}. The broken line shows the thiol quantum yield ϕ_{XH_2}.

Fig. 2. Photodecomposition quantum yield of xanthione as a function of xanthione concentration in MCH. See caption of Fig. 1 for details. The following rate constants were used: $k_H = 1.2 \times 10^4$ M^{-1} s^{-1}; $k_Q = 8.7 \times 10^9$ M^{-1} s^{-1}; $k_0 = 2.0 \times 10^5$ s^{-1}; $k_{R2} = 8.0 \times 10^9$ M^{-1} s^{-1}; $k_{R1} = 50$ M^{-1} s^{-1}; $k_- = 9.0 \times 10^6$ s^{-1}.

4. Discussion

The experimental results for the photochemical transformation of X from its lowest triplet state ^3X may be accommodated by the following scheme:

$$^3X \xrightarrow{k_T = k_{ISC} + k_p} X_0 \qquad (1)$$

self-quenching

$$^3X + X_0 \xrightarrow{k_Q} 2X_0 \qquad (2)$$

H-abstraction

$$^3X + SH \xrightarrow{k_H} [\dot{X}H + \dot{S}] \qquad (3)$$

recombination

$$[\dot{X}H + \dot{S}] \xrightarrow{k_-} X_0 + SH \qquad (4)$$

escape and thiol formation

$$\begin{matrix}[\dot{X}H + \dot{S}] \\ \dot{X}H + SH\end{matrix} \xrightarrow{k_{R1}} \begin{matrix}\dot{X}H + \dot{S} \\ XH_2 + \dot{S}\end{matrix} \quad (5)$$

dimer radical formation

$$[\dot{X}H + \dot{S}] + X_0 \xrightarrow{k_{R2}} \dot{X}_2H + \dot{S} \quad (6)$$

dimer formation

$$\dot{X}_2H + SH \longrightarrow X_2H_2 + \dot{S} \quad (7)$$

Here X_0 represents the ground state xanthione molecule and SH a hydrogen donating solvent molecule; the cage is indicated by a bracket.

4.1. Primary photochemical step

After excitation into the $S_2(\pi\pi^*) \leftarrow S_0$ ($\epsilon(40\,000) = 16\,000\ M^{-1}\ cm^{-1}$ in ethanol) or $S_1(n\pi^*) \leftarrow S_0$ ($\epsilon(16\,000) = 12$) transition of xanthione [7, 8] the excitation energy is channelled into the lowest triplet state $T_1(n\pi^*)$ with a quantum yield of unity [8, 13]. In an aprotic solvent such as 3-MP the decay of this state is governed by radiationless processes to the ground state with $k_0 = 3.7 \times 10^5\ s^{-1}$ at room temperature and at low xanthione concentration (less than 10^{-6} M) *cf.* eqn. (1). At higher concentrations a diffusion-controlled quenching by ground state xanthione molecules, which is physical in nature [10] (eqn. (2)) dominates triplet deactivation. Some pertinent values of the quenching constant k_Q are listed in Table 1. In alcoholic solvents an additional important deactivation route is operative as indicated by a significantly increased k_0 relative to aprotic solvents. This effect, which is accompanied by an increased ϕ_X, is most pronounced in isopropyl alcohol. It is attributed to hydrogen bonding and hydrogen abstraction from the solvent (eqn. (3)). Under these conditions, the triplet decay constant at infinite dilution becomes $k_0 = k_T + k_H[SH]$, where k_H is the rate constant of hydrogen abstraction and k_T the unimolecular triplet constant in hydrogen bonding solvents.

At room temperature the k_0 values in ethanol and i-PrOH are 3 - 6 times larger than are those in 3-MP or acetonitrile. Yet at 77 K, where $\phi_X = 0$, the triplet lifetimes are equal in 3-MP and ethanol. Evidently hydrogen abstraction is ineffective in a matrix at low temperature. The abstraction reaction apparently involves an activation energy and/or a specific steric orientation between the xanthione triplet molecule and the solvent molecule which is not favoured in a rigid matrix. To estimate the upper limit of k_H (293 K) in ethanol, we make the extreme assumption that hydrogen abstraction in methanol is negligible. Thus the decay in methanol is similar to that in ethanol but without hydrogen abstraction, so that $k_m(EtOH) - k_m(MeOH) = k_H[SH] = 3.4 \times 10^5\ s^{-1}$ and $k_H = 2 \times 10^4\ M^{-1}\ s^{-1}$. The quantum yield

of hydrogen abstraction is then $\phi_X(\text{EtOH}) = \phi_{ISC} k_H [SH]/k_0 \geq 0.3$. We find, however, $\phi_X(\text{EtOH}) \approx 0.05$ as the xanthione concentration approaches zero (see Fig. 1). This discrepancy leads us to conclude that radical recombination occurs as indicated in step (3).

The thioketyl radical ($\dot{X}H$) and the solvent radical ($\dot{S}$) are initially caged. Radical recombination and competing consecutive radical reactions govern the decay of the caged radical pair [15, 16]. The behaviour of ϕ_X indicates that radical recombination is an important decay route in ethanol at room temperature.

4.2. Following steps

Apart from the primary photochemical step, a bimolecular reaction involving xanthione ground state molecules must play an important role in the photochemical transformation. This conclusion is inferred from the observation that ϕ_X is strongly dependent on the xanthione concentration (see Figs. 1 and 2). This behaviour of the decomposition quantum yield suggests that after hydrogen abstraction a relatively short-lived intermediate, represented by the caged radical pair, is formed which either decays to the ground state xanthione molecule or reacts further with an X_0 molecule. The higher the X_0 concentration, the higher is the probability that during the lifetime of the caged radical pair an X_0 molecule "penetrates" the cage and comes into the reaction sphere of $\dot{X}H$, forming $\dot{X}_2H$ (eqn. (6)). In a final, probably slow, step (eqn. (7)) this dimeric radical abstracts a second hydrogen atom from a solvent molecule to form the stable photoproduct X_2H_2. The variation of ϕ_X with $[X_0]$ in ethanol at low concentration (Fig. 1) indicates that ϕ_X reaches a limiting value of about 0.05. Although it is apparently quite inefficient, photodecomposition also takes place without the bimolecular step (eqn. (6)). At low xanthione concentration, where the mean collision time between an X_0 molecule and a caged radical pair is long, the XH radical may escape from the cage and abstract a hydrogen atom from a solvent molecule (eqn. (5)). In MCH (Fig. 2) this minor photochemical path, which leads to xanthenyl thiol (XH_2), appears to be negligible.

The formulation of steps (6) and (7) was guided by the mass spectrometric analysis and on previous photochemical results for saturated thiones [1, 2, 5] and thiobenzophenone [1 - 4]. Based on these findings the following structures of the intermediates and product are proposed:

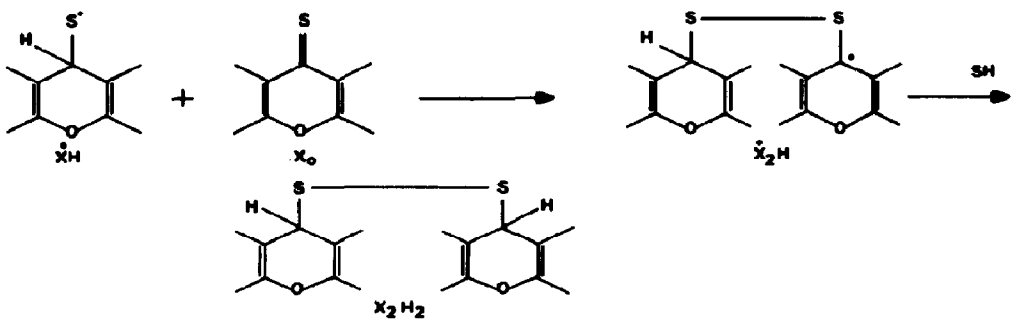

The photolysis products of X in ethanol give rise to a fragment with a mass peak of 181. This mass, which appears at 182 for the photolysis in ethanol-d_6, is assigned to the fragment I:

I

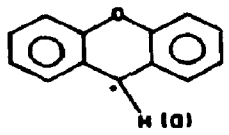

In analogy to the findings with α-mercaptotoluene and dibenzyl disulphide [17], the xanthenyl radical I is considered to be formed from dixanthenyl disulphide (X_2H_2) or xanthenyl thiol (XH_2) by the loss of S_2 or —SH respectively. Although we did not succeed in isolating the final products X_2H_2 and XH_2 owing to their instability, the UV spectrum of a photolysed sample, which shows maxima at 34 250 cm^{-1} (ϵ = 6000 M^{-1} cm^{-1}) and 40 500 cm^{-1} (ϵ = 16 000), provides some structural information.

The main product X_2H_2, to which those considerations are limited, consists of two chromophores, namely the xanthenyl moiety and the disulphide group. Xanthene in ethanol [18] shows absorption maxima at 34 360 cm^{-1} (ϵ = 1730), 35 460 cm^{-1} (ϵ = 2150) and 40 650 cm^{-1} (ϵ = 7410), while dimethyl disulphide [18] has only a weak absorption at 39 300 cm^{-1} (ϵ = 275). The absorption bands of the product appear at almost the same energies. With the expectation that for the X_2H_2 molecule the ϵ values will be approximately twice as large as they are for xanthene (the contribution of the disulphide group is neglected), the observed absorption spectrum is also quantitatively consistent with the proposed product.

4.3. Determination of the rate parameters

To elucidate the rate parameters for the proposed mechanism, the variation of ϕ_X with $[X_0]$ as given in Figs. 1 and 2, was analysed. The decomposition quantum yield expressed in terms of the pertinent rate parameter is then

$$\phi_X([X_0]) = \frac{k_H[SH]}{k_0 + k_Q[X_0]} \frac{k_{R1}[SH] + 2k_{R2}[X_0]}{k_{R1}[SH] + k_{R2}[X_0] + k_-} \tag{8}$$

with

$$k_0 = k_{ISC} + k_p + k_H[SH]$$

The simulation of ϕ_X as a function of [X] is based on the following considerations. Step (6) involves the diffusion of an X_0 molecule to the caged radical pair followed by a radical reaction which, in general, is associated with a low activation energy. Thus k_{R2} may be as large as the rate constant for a diffusion-controlled reaction and its lower limit was taken as 10^8 M^{-1} s^{-1}. Based on the measured k_m values in ethanol, a range of k_H between 10^4 - 6 × 10^4 M^{-1} s^{-1} was explored. By varying k_H, k_- and k_{R2} the best fit for $\phi_X([X_0])$ in ethanol (solid curve in Fig. 1) was obtained with k_H =

1.1×10^4 M^{-1} s^{-1}, $k_- = 1.7 \times 10^5$ s^{-1}, $k_{R1} = 6 \times 10^3$ M^{-1} s^{-1} and $k_{R2} = 6 \times 10^9$ M^{-1} s^{-1}. The experimental data in MCH were best reproduced with $k_H = 1.2 \times 10^4$ M^{-1} s^{-1}, $k_- = 9.0 \times 10^6$ s^{-1}, $k_{R1} \approx 0$ and $k_{R2} = 8 \times 10^9$ M^{-1} s^{-1}.

These rate constants are very reasonable. The k_{R2} values in both solvents are close to those for diffusion-controlled reactions and k_H is as expected similar in ethanol and MCH. However, the calculated value of $k_H = 1.1 \times 10^4$ M^{-1} s^{-1} in ethanol, which is not far from the estimated lower limit of approximately 2×10^4 M^{-1} s^{-1} (see earlier) suggests that the significantly higher k_0 value in ethanol than in aprotic solvents is not mainly due to hydrogen abstraction. Rather, the enhanced k_0 value in methanol and ethanol is probably due to hydrogen bonding between the thioketone group and the solvent. The 25% reduction of k_0 between ethanol and ethanol-d_1 while ϕ_X remains unchanged (see Table 1) is consistent with this suggestion.

Despite almost identical k_H values, ϕ_X in MCH is about an order of magnitude smaller than it is in ethanol. Owing to the large rate constant for radical recombination which dominates the decay of the caged radical [15, 16], ϕ_X in MCH remains low. The calculated kinetic data permit the lifetimes of the caged radical pair to be estimated as about 5 μs in ethanol and about 100 ns in MCH. Assuming that the cage stability for an uncharged radical pair is mainly determined by the solvent structure [16] it is attractive to speculate that the significantly larger lifetime in ethanol is due to hydrogen bonding between solvent molecules [19].

The quantum yield ϕ_X is, within experimental error, the same in ethanol-d_1 as it is in ethanol. In fully deuterated ethanol ϕ_X is reduced by a factor of about 16. Since k_0 is the same in both deuterated solvents, hydrogen and deuterium abstraction from the α position of ethanol are apparently equally efficient, *i.e.* $k_H \approx k_D$. The dramatically reduced ϕ_X value in ethanol-d_6 is probably due to a much higher rate constant for radical recombination (eqn. (4)) when deuterated radicals are involved.

Acknowledgment

Support of this work by the Deutsche Forschungsgemeinschaft and the Verband der Deutschen Chemischen Industrie is greatly appreciated. Many thanks are due to Prof. Karl Weiss, Boston, for critically reading the manuscript, and to Dr. M. Mahaney, Mrs. E. Kayser and Mr. R. Barreca for technical assistance.

References

1 P. de Mayo, Acc. Chem. Res., 9 (1976) 52.
2 D. Paquer, Int. J. Sulfur Chem., 8 (1973) 173.
3 G. Oster, L. Citarel and M. Goodman, J. Am. Chem. Soc., 84 (1962) 703.
A. Ohno and N. Kito, Int. J. Sulfur Chem., Part A, 1 (1971) 26.
4 D. R. Kemp and P. de Mayo, Chem. Commun., (1972) 233.

5 K. Y. Law, P. de Mayo and S. K. Wong, J. Am. Chem. Soc., 99 (1977) 5813.
J. C. Scaiano, J. P.-A. Tremblay and K. U. Ingold, Can. J.. Chem., 54 (1976) 3407.
J. R. Bolton, K. S. Chen, A. H. Lawrence and P. de Mayo, J. Am. Chem. Soc., 97 (1975) 1832.
6 A. H. Lawrence, C. C. Liao, P. de Mayo and V. Ramamurthy, J. Am. Chem. Soc., 98 (1976) 3572.
N. J. Turro and V. Ramamurthy, Tetrahedron Lett., 28 (1976) 2423.
A. Couture, K. Ho, M. Hashino, P. de Mayo, R. Suau and W. R. Ware, J. Am. Chem. Soc., 98 (1976) 6218.
H. Gotthardt and S. Nieberl, Tetrahedron Lett., 39 (1976) 3563.
H. Gotthardt, Tetrahedron Lett., 34 (1971) 2345.
7 D. A. Capitanio, H. J. Pownall and J. R. Huber, J. Photochem., 3 (1974) 225.
M. Mahaney and J. R. Huber, J. Photochem., 5 (1976) 333.
8 M. Mahaney and J. R. Huber, Chem. Phys., 9 (1975) 371.
R. W. Anderson, R. M. Hochstrasser and H. J. Pownall, Chem. Phys. Lett., 43 (1976) 224.
9 G. Maki, P. Svejda and J. R. Huber, Chem. Phys., 32 (1978) 369.
10 U. Brühlmann and J. R. Huber, Chem. Phys. Lett., 54 (1978) 606.
11 F. W. Arndt and L. Lorenz, Ber., 63 (1930) 3129.
12 C. G. Hatchard and C. A. Parker, Proc. R. Soc. London, Ser. A, 235 (1956) 518.
13 O. Serafimov, U. Brühlmann and J. R. Huber, Ber. Bunsenges. Phys. Chem., 79 (1975) 202.
O. Serafimov, H. J. Haink and J. R. Huber, Ber. Bunsenges. Phys. Chem., 80 (1976) 536.
14 S. J. Formosinho, J. Chem. Soc., Faraday Trans. 2, 72 (1976) 1332.
J. C. Scaiano, J. Photochem., 2 (1973/74) 81.
15 C. Richard and P. Granger, in P. Diehl *et al.* (eds.), NMR Basic Principles and Progress, Vol. 8, Springer, Berlin, 1974.
M. R. Topp, Chem. Phys. Lett., 32 (1975) 144.
M. V. Encina and E. A. Lissi, J. Photochem., 8 (1978) 131.
16 O. Dobis, J. Chem. Phys., 65 (1976) 4264.
Th. Koenig and H. P. Fischer, "Cage" effects. In J. K. Kochi (ed.), Free Radicals, Vol. I, Wiley, New York, 1973.
17 J. G. Grassell (ed.), CRC Atlas of Spectral Data and Physical Constants of Organic Compounds, CRC Press, Cleveland, 1973.
18 DMS-UV Atlas of Organic Compounds, Butterworths, London, 1971.
19 G. C. Pimentel and A. L. McClellan, The Hydrogen Bond, Freeman, San Francisco, 1960.